Very Strong Bainite

F. G. Caballero [a] and H. K. D. H Bhadeshia [b]

[a] Department of Physical Metallurgy, Centro Nacional de Investigaciones Metalúrgicas (CENIM), Consejo Superior de Investigaciones Científicas (CSIC), Avda. Gregorio del Amo, 8, 28040 Madrid, Spain. fgc@cenim.csic.es

[b] Department of Materials Science and Metallurgy, University of Cambridge, Pembroke Street, Cambridge CB2 3QZ, U. K. hkdb@cus.cam.ac.uk

Abstract

Steel with an ultimate tensile strength of 2500 MPa, a hardness at 600-670 HV and toughness in excess of 30-40 MPa $m^{1/2}$ is the result of exciting new developments with bainite. The simple process route involved avoids rapid cooling so that residual stresses can in principle be avoided even in large pieces. The microstructure is generated at temperatures which are so low that the diffusion of iron is inconceivable during the course of the transformation to bainite. As a result, slender plates of ferrite, just 20-40 nm thick are generated, giving rise to the extraordinary properties.

Keywords: bainite; retained austenite; steels; phase transformations, strength

1. Introduction

Strength is a term which needs to be used with care. A material can be made stronger by reducing its size in order to avoid defects; carbon nanotubes fall into this category since their strength collapses as they are made into ropes with dimensions in the micrometer scale [1]. Alternatively, strength can be achieved by packing the material with defects that interfere with the motion of dislocations; *Scifer*, which has a strength of 5.5 GPa is made in this way [2]. However, the deformation process by which the defects are introduced places limits on the dimensions in which the material can be produced. Thus, *Scifer* can only be produced in the form of wires whose diameters are measured in micrometers.

Another method of making strong materials is to reduce the scale of the microstructure using heat treatment. The giga-pascal steels rely for their strength on fine martensitic microstructures which are generated during rapid cooling [3,4]. This also limits the size of the components that can be produced with uniform properties.

In this article we review a novel method for making extremely strong and cheap nanocrystalline-steel without using deformation, rapid heat-treatment or mechanical processing. Furthermore, the material can be produced in a form which is large in all its three dimensions, and has a plethora of other properties useful in engineering design. The new material relies on a microstructure called *bainite*, which has been known of since 1930 [5]; the novelty is in the alloy design which leads to the fine scale and controlled response to heat treatment.

2. Blueprint for Alloy Design

It has long been known that alloying a steel with about 2 wt% of silicon can in appropriate circumstances yield a carbide-free microstructure which is a mixture of bainitic ferrite and carbon-enriched residual austenite. The silicon does not dissolve in cementite and hence suppresses its precipitation from austenite. Cementite is a cleavage and void-initiating phase which is best eliminated from strong steels. However, the full benefits of this carbide-free bainitic microstructure have frequently not been realised. This is because the transformation to baintic ferrite stops well before equilibrium is reached [6-9]. There remain large regions of untransformed austenite which under stress decompose to hard, brittle martensite.

The problem, which is essentially thermodynamic in origin, can be solved by altering the relative stabilities of the austenite and ferrite phases. The essential principles governing the optimisation of such microstructures are now well established. Everything must be done that encourages an increase in the amount of bainitic ferrite so as to consume the blocks of austenite [10,11]. With careful design, impressive combinations of strength and toughness have been reported for high-silicon bainitic steels [10-14]. More recently, it has been demonstrated experimentally that models based on the atomic mechanism of displacive transformation, can be applied successfully to the design of carbide-free bainitic steels, the only experiments needed are those to validate the theoretical predictions [15,16]. Toughness values of nearly 130 MPa $m^{1/2}$ were obtained for strength in the range of 1600-1700 MPa. This compares well with maraging steels, which are at least ninety times more expensive.

The details of the design method, which is based on the discipline with which the atoms move during transformation, are as follows.

Bainite grows without diffusion in the form of tiny plates known as ‘sub-units’; each plate grows to a limited size which is determined by the plastic accommodation of the shape deformation accompanying transformation. One consequence of diffusionless growth is that the plates can be supersaturated with carbon, in which case the carbon partitions into the

residual austenite soon after the growth event. Diffusionless growth of this kind can only occur if the carbon concentration of the parent austenite is less than that given by the T_o' curve. The T_o curve is the locus of all points, on a temperature versus carbon concentration plot, where austenite and ferrite of the same chemical composition have the same free energy. The T_o' curve is defined similarly but taking into account the stored energy of the ferrite due to the displacive mechanism of transformation.

It follows that the maximum amount of bainitic ferrite that can form in the absence of carbide precipitation is limited by the T_o' curve; this is a severe limitation if large quantities of blocky austenite remain in the microstructure at the point where transformation stops. The design procedure avoids this difficulty in three ways: by adjusting the T_o curve to greater carbon concentrations using substitutional solutes, by controlling the mean carbon concentration, and by minimising the transformation temperature.

It is worth pointing out that attempts have been made to interpret the T_o criterion differently. One theory argues that the reason why the bainite reaction stops prematurely is because of the plastic work done as the plate grows by a displacive mechanism overwhelms the driving force for transformation [17,18]. However, the theory is derived incorrectly in that the calculated work is divided by the fraction of remaining austenite, whereas it is in fact per unit quantity of bainite. Furthermore, there is an upper limit to the amount of work done in plastic accommodation [19]; this is the strain energy associated with an elastically accommodated plate, amounting to just 400 J mol^{-1} [20]. A alternative interpretation [21] requires local equilibrium at the interface, contradicting atomic resolution experiments which show the absence of substitutional solute partitioning [23].

Returning now to the design, it is known that blocky austenite should be avoided to ensure good toughness. The size of these blocks (which may transform to brittle martensite under stress) must be less than or comparable to that of other fracture initiating phases such as non-

metallic inclusions. A reduction in the scale of the microstructure enhances both strength and toughness; this leads naturally to the conclusion that the microstructure is best generated at low temperatures. The question then arises, what is the lowest temperature at which bainite can be obtained?.

3. Low Transformation-Temperature

In order to answer this question, it is necessary to be able to reliably calculate the highest temperature at which bainite can form. This requires a consideration of both nucleation and growth.

Bainite can only form below the T_o' temperature when

$$\Delta G^{\gamma\rightarrow\alpha} < -G_{SB} \text{ and } \Delta G_m < G_N \qquad (1)$$

where $G_{SB} \cong 400$ J mol^{-1} is the stored energy of bainite [24]; $\Delta G^{\gamma\rightarrow\alpha}$ is the free energy change accompanying the transformation of austenite without any change in chemical composition. The first condition therefore describes the limit to growth. The second condition refers to nucleation; thus, ΔG_m is the maximum molar Gibbs free energy change accompanying the nucleation of bainite . G_N is a universal nucleation function based on a dislocation mechanism of the kind associated with martensite [24-26]. The variation of G_N with temperature is well-behaved even for the high carbon steels of interest here [27]. Together with the growth condition, the function allows the calculation of the bainite start temperature, B_s, from a knowledge of thermodynamics alone. An example calculation is

presented in Figure 1a, which reveals the important result that extraordinarily low transformation temperatures can be achieved because the bainite and martensite-start temperatures remain separated.

The rate of reaction is also important since transformation must be achieved in a realistic time. For this purpose, a method [9] developed to allow the estimation of isothermal transformation diagrams can be used, with the chemical composition as an input. Calculated time-temperature-transformation (TTT) diagrams indicate the time required to initiate transformation (Figure 1b). Such calculations also help design the hardenability of the alloy so as to avoid interfering reactions such as allotriomorphic ferrite and pearlite.

4. The Alloys

Low transformation temperatures are associated with fine microstructures which in turn possess strength and toughness. The theory described above has been used to develop steels which transform to bainite at temperatures as low as 125 ºC, in time scales which are practical (Table 1). The low B_S temperature is a consequence of the high carbon concentration and to a lesser extent, solutes such as manganese, chromium which in the present context increase the stability of austenite relative to ferrite. The molybdenum is added to ameliorate any temper-embrittlement phenomena due to inevitable impurities such as phosphorus. The alloys all contain sufficient silicon to suppress the precipitation of cementite from any austenite.

In the steels designated A and B (Table 1), bainite can take between 2 to some 60 days to complete transformation within the temperature range 125-325 ºC [28,29]. In a commercial scenario it may be useful to accelerate transformation without losing the ability to utilise low temperatures. Certain elements increase the free energy change when austenite transforms and

hence should accelerate its decomposition; hence, the cobalt and aluminium containing alloys in Table 1.

Some micrographs following isothermal transformation to bainitic ferrite in the temperature range 125-325 ^{o}C are illustrated in Figure 2, for alloy A. The early stage of transformation is shown in Fig 2a for a sample isothermally heat treated for 25 days at 125 ºC. As Fig. 2b suggests, only a small fraction of bainite (~0.10) is formed after 30 days of holding time at 150 ºC. Very long heat treatments are required (more than 2 months) to obtain substantial transformation when the temperature is as low as 125 ºC or 150 ºC. The rate of transformation is faster when the temperature exceeds 150 °C. Thus, it is found that the fraction of bainite is 0.6 for transformation at 190 and 250 ºC for 7 days and 24 hours, respectively (Figs. 2c and 2d). An almost fully bainitic microstructure (~90 % bainite) is obtained at 190 ºC after 9 days of transformation. At 300 ºC, the maximum volume fraction of bainite formed was 0.6 and 4 days were needed to complete the transformation.

The calculated [9,30,31] time-temperature-transformation (TTT) diagram for the initiation of transformation in Steels A and B are shown in Fig. 3, which also contains experimental data for the reaction times. The upper C-curve represents the onset of reconstructive transformations such as allotriomorphic ferrite and pearlite, whereas the lower curve is for bainite. The measured values for a detectable degree of transformation are in reasonable agreement with those calculated, except at the highest temperature where the time period required is underestimated.

X-ray analysis was used to estimate the quantities of retained austenite present at the point where transformation ceases (Fig. 4). The retained austenite fraction is expected to increase for the higher transformation temperature because less bainite forms; this is in contrast to the situation with low-carbon alloys, where a larger fraction of bainite favours the retention of austenite because of the portioning of carbon into the austenite.

The maximum amount of bainite that can be obtained at any temperature is limited because the carbon content of the residual austenite must not exceed that given by the T_o' curve. At that point, the enriched austenite can no longer transform into bainite. The carbon concentrations of the austenite and bainitic ferrite, determined using X-ray analysis in Steels A and B are presented in Fig. 4b. The fact that the measured concentrations in austenite lie between the T_o' and the paraequilibrium Ae_3 phase boundaries for both steels is consistent with a mechanism in which the bainite grows without any diffusion, but with excess carbon partitioning into the austenite soon after transformation. The reaction is said to be *incomplete* since transformation stops before the phases achieve their equilibrium compositions.

The X-ray data also indicate that excess carbon is trapped in the bainitic ferrite (Fig. 4b) and the results have been verified using an atom probe [32]. The latter technique revealed a distribution of carbon concentrations in bainitic ferrite (Fig. 4c). It is believed that the carbon is retained in the ferrite because it is trapped at defects.

The transmission electron micrograph in Fig. 5 illustrates a typical microstructure of low-temperature bainite, with slender plates which are incredibly thin and long, giving a most elegant fine scale structure which is an intimate mixture of austenite and ferrite. Dislocation debris is evident in both the bainitic ferrite and the surrounding austenite. Extensive transmission microscopy failed to reveal carbides in the microstructure, only a few minute (20 nm wide and 175 nm long) cementite particles in the ferrite within Steel A transformed at 190 ºC for 2 weeks [28]. Quite remarkably, the plates formed at 200 ºC in Steel B (Fig. 5) have a width that is less than 50 nm, with each plate separated by an even finer film of retained austenite. It is this fine scale which is responsible for much of the tenacity of the microstructure, with hardness values in excess of 600 HV and strength in excess of 2.5 GPa [28]. The dispersion of films of austenite undoubtedly helps render the steel tough.

Analysis indicates that the largest effects on plate thickness are the strength of the austenite, the free energy change accompanying transformation and a small independent effect due to transformation temperature [33]. In the present case, the observed refinement is a consequence mainly of high carbon content and the low transformation temperature on enhancing the strength of the austenite.

5. Acceleration of transformation

Slow transformation gives the ability to transform large components to a uniform microstructure free from residual stresses or complex processing. Suppose, however, that there is a need for more rapid heat-treatment. The transformation can easily be accelerated to complete the processing within hours (as opposed to days), by making controlled additions of small quantities of solutes to the steel, such that the free energy change as austenite changes into ferrite is enhanced. There are essentially two choices, aluminium and cobalt, in concentrations less than 2 wt%, have been shown to accelerate the transformation in the manner described [34]. Both are effective, either on their own or in combination. They work by increasing the driving force for the transformation of austenite; they have therefore been added to make Steels C and D which should then transform more rapidly. Fig. 6.a shows the increase in the reaction rate due to the cobalt, the effect is particularly large when both elements are added. A further rate increment is possible by refining the austenite grain size (Fig. 6.b). An increase in the free energy change also means that a greater fraction of bainite is obtained, which may have the additional advantage of increasing the stability of the austenite [34].

6. Tempering Resistance

Bainite tempers more gently than martensite because it *autotempers* as it forms. Its starting hardness is less than that of martensite, so it follows that any change in hardness must be small when compared with martensite. However, the starting hardness of the low-temperature bainite described here is very high, so it is of interest to study its tempering behaviour [35]. Figure 7 shows a plot of the normalised hardness of a variety of steels versus the tempering parameter defined as $T(20+\log t)$ where T is expressed in Kelvin and t in hours. The normalised hardness is given by $(H-H_{\min})/(H_{\max}-H_{\min})$, where H, H_{max} and H_{min} represent the hardness, untempered hardness and fully-softened hardness, respectively. The tempering resistance of the baintic steel is impressive when compared against an equivalent martensitic or secondary hardening steel. The mild secondary hardening effect in Steel B is associated to with the intense precipitation of fine cementite when the retained austenite decomposes. Furthermore, these the precipitation occurs at the boundaries of the ferrite plates, thus pinning them and preventing coarsening. Since much of the strength of the bainite comes from the plate size, the microstructure becomes very resistant to tempering.

It is also found that the excess carbon within the ferrite remains there during heat treatment, reducing only in proportion to the density of defects [35].

7. High Strain Rate Deformation

Ballistic experiments conducted at strain rates of about 10^7 s^{-1} have revealed that bainitic steel with a composition and microstructure similar to that of steel A (Table1) undergoes a

pressure induced martensitic phase transformation to epsilon-iron (hexagonal close-packed) at about 13 GPa [36]. This is as would be expected from the phase diagram [37]. Strength is expected to increase with strain rate; the experiments indicate a yield strength in the range 3.5-10 GPa under ballistic conditions. The spall strength, a parameter important in the design of armour, is found to be about about 2 GPa, decreasing sharply as the longitudinal stress approaches the 13 GPa associated with the phase transition. As explained by the authors, the basis of the latter correlation is not clear.

Conclusions

It is clear that bainite can be obtained by transforming at very low temperatures. There is then no possibility that iron or substitutional solutes diffuse. A consequence of the low transformation temperature is that the plates of bainite are incredible fine, 20-40 nm thick, making the material very strong. This is a bulk nanocrystalline material that is cheap and can be obtained without severe processing. When this feature is combined with the fact that the plates of ferrite are interspersed with austenite, it becomes possible to create novel strong and tough steels. The potential for exploitation is large because the alloys are routine to manufacture.

The alloys designed so far either transform slowly over a period of many days, or have to be alloyed with cobalt and aluminium in order to accelerate transformation. In the future, it is possible that rapid transformation could be engineered by controlling the manganese concentration. The key will be to do this without compromising properties.

Acknowledgements

F.G. Caballero would like to thank Spanish Ministerio de Ciencia y Tecnología for the financial support in the form of a Ramón y Cajal contract (Programa RyC 2002).

References

1. Yu MF, Files BS, Arepalli S, Ruoff RS. Tensile loading of ropes of single wall carbon nanotubes and their mechanical properties. Phys Rev Lett 2000; 84: 5552-5555.
2. Bhadeshia HKDH, Harada H. High-strength (5 GPa) steel wire - an atom-probe study. Appl Surf Sci 1993; 63: 328-333.
3. Olson GB, Azrin M, Wright ES. Innovations in Ultrahigh-Strength Steel Technology, New York: Sagamore Army Materials Research, 1987; 34: 1-765.
4. Bhadeshia HKDH. Large chunks of very strong steel. Millenium Steel 2004; 5: 25-28.
5. Davenport ES, Bain EC. Transformation of austenite at constant subcritical temperatures. Trans. Met. Soc. AIME 1930; 90: 117-154.
6. Bhadeshia HKDH, Waugh AR. Bainite - an atom-probe study of the incomplete reaction phenomenon. Acta Metall 1982; 30: 775-784.
7. Chang LC, Bhadeshia HKDH. Carbon concentration of retained austenite in isothermally. Transformed 300M Steel" Mat Sci Eng A 1994; A184: L17-20.
8. Self P, Bhadeshia HKDH, Stobbs M. Lattice spacings from lattice fringes. Ultramicroscopy 1981; 6: 29-40.
9. Bhadeshia HKDH. A thermodynamic analysis of isothermal transformation diagrams. Metal Sci 1982; 16: 159-165.
10. Bhadeshia HKDH, Edmonds DV. Bainite in silicon steels: a new composition-property approach. Part I. Metal Sci 1983; 17: 411-419.

11. Bhadeshia HKDH, Edmonds DV. Bainite in silicon steels: a new composition-property approach. Part II. Metal Sci 1983; 17: 420-425.
12. Miihkinen VTTD, Edmonds DV. Microstructural examination of 2 experimental high-strength bainitic low-alloy steels containing silicon. Mater Sci Tech Lond 1987; 3: 422-431.
13. Miihkinen VTTD, Edmonds DV. Tensile deformation of 2 experimental high-strength bainitic low-alloy steels containing silicon. Mater Sci Tech Lond 1987; 3: 432-440.
14. Miihkinen VTTD, Edmonds DV. Fracture-toughness of 2 experimental high-strength bainitic low-alloy steels containing silicon. Mater Sci Tech Lond 1987; 3: 441-449.
15. Caballero FG, Bhadeshia HKDHK, Mawella JA, Jones DG, Brown P. Design of novel high-strength bainitic steels: Part I. Mater Sci Tech Lond 2001; 17: 512-516.
16. Caballero FG, Bhadeshia HKDHK, Mawella JA, Jones DG, Brown P. Design of novel high-strength bainitic steels: Part II. Mater Sci Tech Lond 2001; 17: 517-522.
17. Bouaziz O, Quidort D, Maugis P. Bainite transformation stasis controlled by plastic work in austenite. Rev Metall Paris 2003; 100: 103-108.
18. Quidort D, Bouaziz O. The bainite transformation stage in the processing of Trip-Aided sheet steels. Can Metall Quart 2004; 43: 25-33.
19. Christian JW. Proc. ICOMAT 1979, Masschusetts: MIT Press, 1979: 220-234.
20. Bhadeshia HKDHK. Developments in martensitic and bainitic steels: role of the shape deformation. Mat Sci Eng A 2004; A378: 34-39.
21. Hillert M. The nature of bainite. ISIJ Int 1995; 35: 1134-1140.
22. Bhadeshia HKDH, Waugh AR. An atom-probe study of Bainite. In: Proc. Int. Conf. Solid-Solid Phase Trans., Warrendale: Metall. Soc. AIME, 1981: 993-998.

23. Stark I, Smith GDW, Bhadeshia HKDH. The element redistribution associated with the incomplete-reaction phenomenon in bainitic steels: an atom-probe investigation. In: Proc. Int. Conf. Solid-Solid Phase Trans., London: Inst. of Metals, 1988: 211-215.
24. Bhadeshia HKDH. A rationalisation of shear transformations in steels. Acta Metall 1981; 29: 1117-1130.
25. Bhadeshia HKDH. Bainite in steels, 2nd ed. London: Institute of Materials, 2001.
26. Olson GB, Cohen M. General mechanism of martensitic nucleation .1. General concepts and fcc-hcp transformation. Metall Trans 1976; 7A: 1897-1923
27. García-Mateo C, Bhadeshia HKDH. Nucleation theory for high-carbon bainite. Mat Sci Eng A 2004; A378: 289-292.
28. Caballero FG, Bhadeshia HKDHK, Mawella JA, Jones DG, Brown P. Very strong low temperature bainite. Mater Sci Tech Lond 2002; 18: 279-284.
29. García-Mateo C, Caballero FG, Bhadeshia HKDH. Hard bainite. ISIJ Int 2003; 43: 1238-1243.
30. Lee JL, Bhadeshia HKDH. A methodology for the prediction of ttt diagrams. Mat Sci Eng A 1993; A171: 223-230.
31. Bhadeshia HKDH. in Materials Algorithms Project http://www.msm.cam.ac.uk/map/steel/programs/mucg46-b.html.
32. Peet M, Babu SS, Miller MK, Bhadeshia HKDH. Three-dimensional atom probe analysis of carbon distribution in low-temperature bainite. Scripta Mater 2004; 50: 1277-1281.
33. Singh SB, Bhadeshia HKDH. Estimation of bainite plate-thickness in low-alloy steels. Mat Sci Eng A 1998; 245: 72-79.
34. García-Mateo C, Caballero FG, Bhadeshia HKDH. Acceleration of low-temperature bainite. ISIJ Int 2003; 43: 1821-1825.

35. García-Mateo C, Peet M, Caballero FG, Bhadeshia HKDH. Tempering of a hard mixture of bainitic ferrite and austenite. Mater Sci Tech Lond 2004; 20: 814-818.
36. Hammond RI, Proud WG. Does the pressure-induced α−ε phase transition occur for low-alloy steels. In: Proc. Mathematical, Physical and Engineering Sciences, The Royal Society, 2004; A460: 2959-2974.
37. Christou A, Brown N. High pressure phase transition and demagnetization in shock compressed Fe-Mn alloys. J Appl Phys 1971; 42: 4160-4170.

Figure Legends

Figure 1: Example calculations: (a) computed martensite-start, M_S, and bainite-start, B_S, temperatures, (b) the time required to initiate transformation.

Figure 2.- Optical micrographs of isothermal decomposition of austenite in Steel A: (a) 125 ºC for 25 days; (b) 150 ºC for 30 days; (c) 190 ºC for 7 days; and (d) 250 ºC for 24 hours.

Figure 3.- Calculated TTT diagram for the initiation of transformation, and measured times for the commencement (filled points) and termination of reaction (open circles): (a) steel A; (b) steel B.

Figure 4.- X-ray experimental data on: (a) volume fractions of retained austenite; and (b) carbon in bainitic ferrite (square symbols) and austenite (circles); (c) carbon distribution in a baintic ferrite plate obtained by 3D-atom probe microanalysis. Calculated curves according to [31].

Figure 5.- Transmission electron micrographs of microstructure obtained at 200 ºC for 15 days in Steel B.

Figure 6.- Isothermal transformation at 200 ºC: (a) austenitisation at 1000 ºC for 15 min; (b) austenitisation at 900 ºC for 30 min. PAGS stands for prior austenite grain size.

Figure 7.- Comparison of the temper resistance of Steel B with that of an Fe-0.5C-1.3Si wt-% quenched and tempered martensitic steel, and a secondary hardening steel (Fe-0.34C-5.08Cr-1.43Mo-0.92V-0.4Mn-1.07Si wt%).

Tables

Table 1 Compositions of new alloys, wt%

Steel	C	Si	Mn	Cr	Mo	V	Co	Al
A	0.79	1.59	1.94	1.33	0.30	0.11	-	-
B	0.98	1.46	1.89	1.26	0.26	0.09	-	-
C	0.83	1.57	1.98	1.02	0.24	-	1.54	-
D	0.78	1.49	1.95	0.97	0.24	-	1.60	0.99

Figures

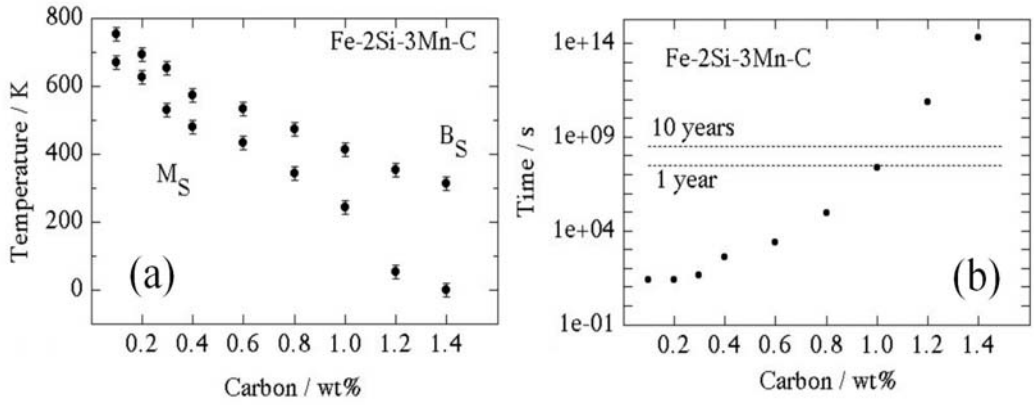

Figure 1: Example calculations: (a) computed martensite-start, M_S, and bainite-start, B_S, temperatures, (b) the time required to initiate transformation.

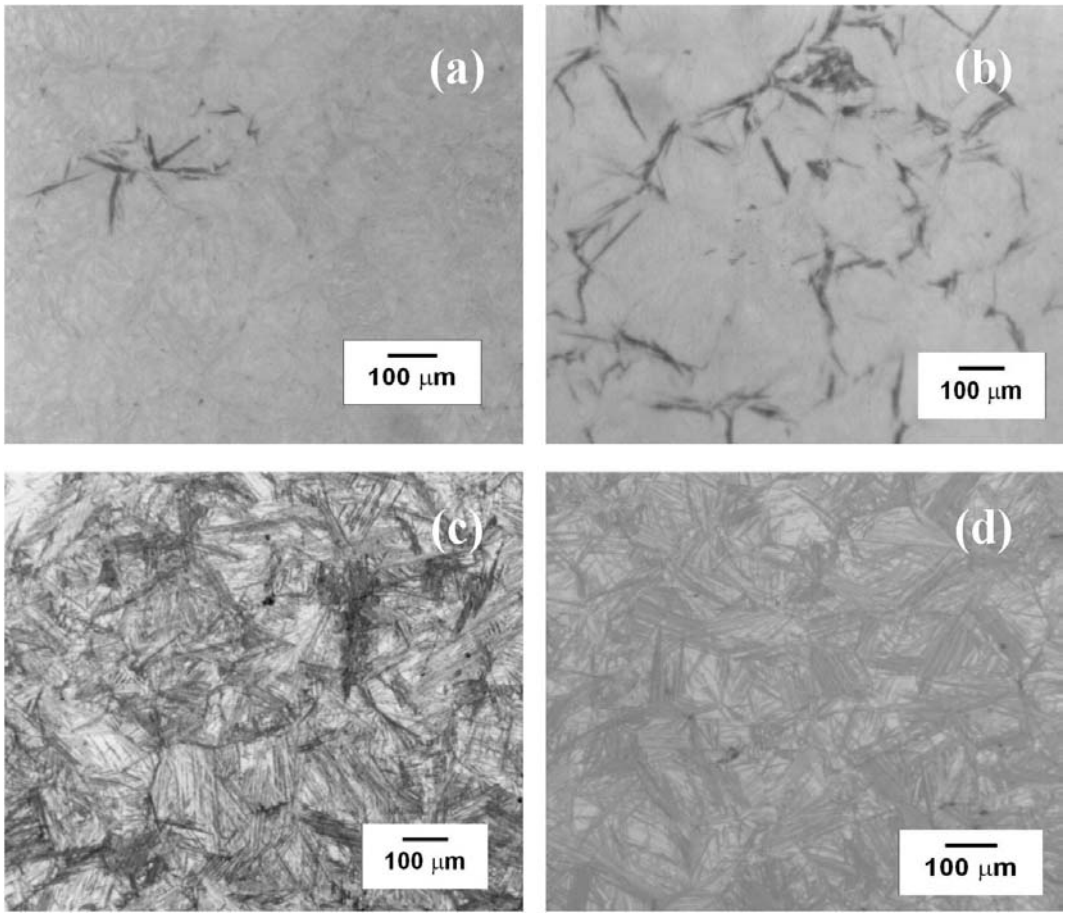

Figure 2.- Optical micrographs of isothermal decomposition of austenite in Steel A: (a) 125 ºC for 25 days; (b) 150 ºC for 30 days; (c) 190 ºC for 7 days; and (d) 250 ºC for 24 hours.

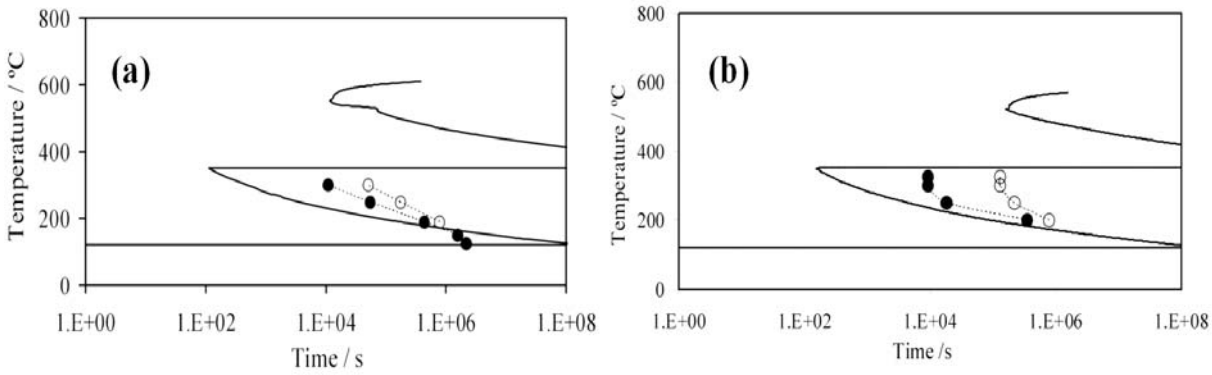

Figure 3.- Calculated TTT diagram for the initiation of transformation, and measured times for the commencement (filled points) and termination of reaction (open circles): (a) steel A; (b) steel B.

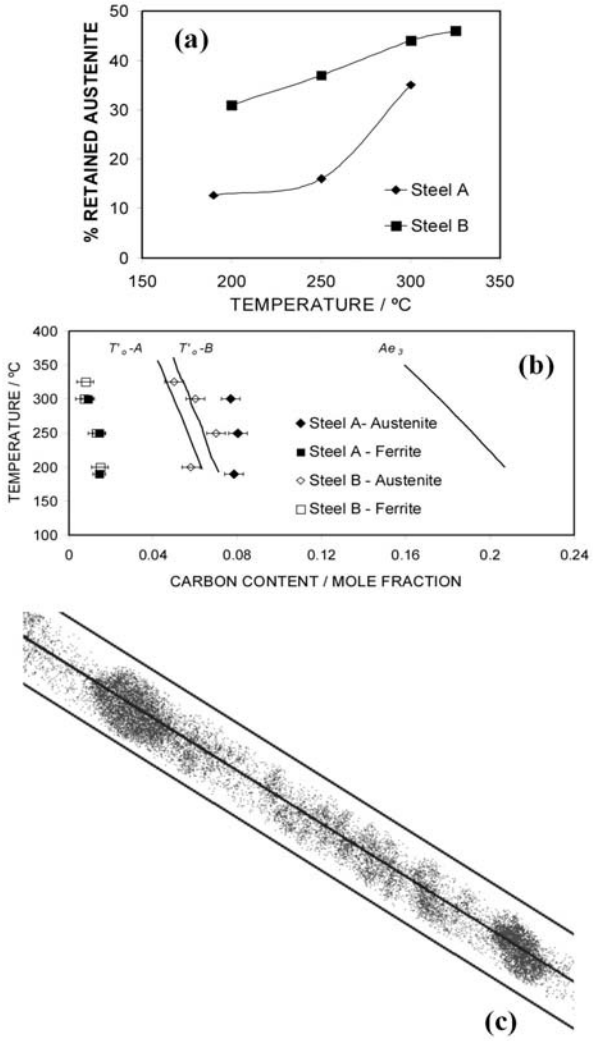

Figure 4.- X-ray experimental data on: (a) volume fractions of retained austenite; and (b) carbon in bainitic ferrite (square symbols) and austenite (circles); (c) carbon distribution in a baintic ferrite plate obtained by 3D-atom probe microanalysis. Calculated curves according to [31].

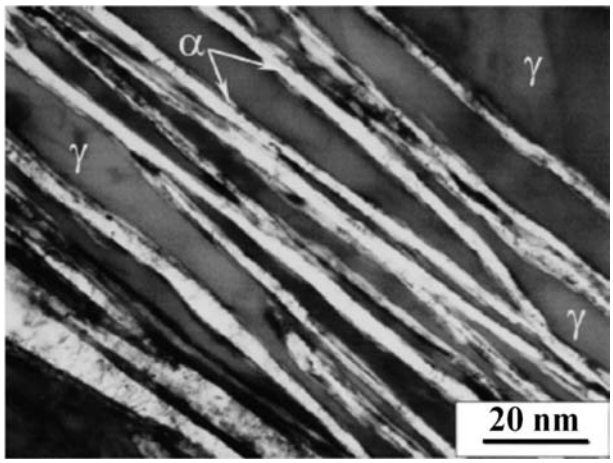

Figure 5.- Transmission electron micrographs of microstructure obtained at 200 ºC for 15 days in Steel B.

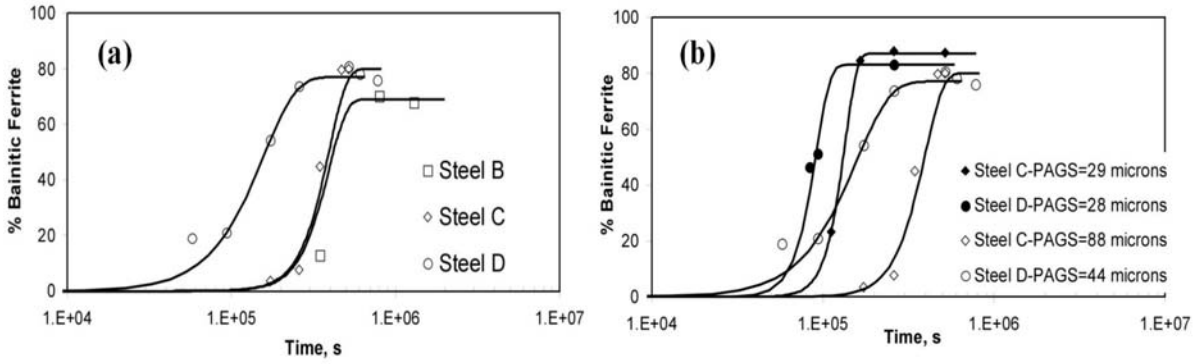

Figure 6.- Isothermal transformation at 200 ºC: (a) austenitisation at 1000 ºC for 15 min; (b) austenitisation at 900 ºC for 30 min. PAGS stands for prior austenite grain size.

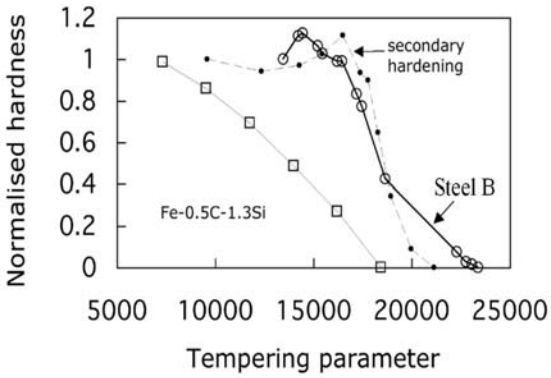

Figure 7.- Comparison of the temper resistance of Steel B with that of an Fe-0.5C-1.3Si wt-% quenched and tempered martensitic steel, and a secondary hardening steel (Fe-0.34C-5.08Cr-1.43Mo-0.92V-0.4Mn-1.07Si wt%).